Electron transfer in bis(hydrazines), a critical test for application of the Marcus model

3 AUTHORS, INCLUDING:

Sven Larsson
Chalmers University of Technology
171 PUBLICATIONS **3,442** CITATIONS

SEE PROFILE

Stephen F Nelsen
University of Wisconsin–Madison
118 PUBLICATIONS **2,249** CITATIONS

SEE PROFILE

Electron Transfer in Bis(hydrazines), a Critical Test for Application of the Marcus Model

FREDRIK BLOMGREN,[1] SVEN LARSSON,[1] STEPHEN F. NELSEN[2]

[1]*Department of Physical Chemistry, Chalmers University of Technology, S-41296 Gothenburg, Sweden*
[2]*Department of Chemistry, University of Wisconsin, 1101 University Avenue, Madison, Wisconsin 53706-1396*

ABSTRACT: Electron transfer in the cations of bis(hydrazines), bridged by six different π-systems (compounds 1–6) is studied using *ab initio* and density functional theory (DFT) methods. Due to ionization from an antibonding combination of the lone-pair orbitals of the nitrogens in one of the hydrazine units, conjugation is introduced in the N—N bond of that unit. This leads to a shortening of the N—N bond distance and an increase of the planarity around the nitrogens. Due to steric hindrance, this causes an increase of the angle, called φ, between the lone-pair orbital on the nitrogen attached to the bridge and the p-orbital on the adjacent bridge carbon for the ionized unit in the charge localized, relaxed state of the molecule. This angle controls the magnitude of the electronic coupling. In the fully delocalized symmetric transition state of the ion, however, this angle is low for both units, due to the fact that the conjugation introduced at the ionized hydrazine unit is now shared between both units. An extended π-system is formed including the orbitals of the hydrazine units and the bridge, which leads to a large electronic coupling. The electronic coupling derived by optical methods, corresponding to the structure of the relaxed, asymmetric cation with a large φ for the ionized unit, appears to be much smaller. We believe this is due to an approximate cosine dependence on φ of the coupling. The calculations carried out support these conclusions.   © 2001 John Wiley & Sons, Inc.   J Comput Chem 22: 655–664, 2001

Keywords: electron transfer; bis(hydrazines); Marcus model

Introduction

Electron transfer (ET) reactions are probably the only chemical reactions for which the rate usually can be calculated with reasonable accuracy for quite large systems. The reason is that the structural changes during the reaction are small, and hence, take place close enough to the potential energy surface (PES) minima to allow a parabolic approximation. The rate may be calculated using the Marcus model,[1, 2] if the force constants (f) for the activating vibration, the reorganization energy (λ) and the average electronic coupling (H_{ad}) at the seam of the avoided crossing between the relevant PESs for ET are known. The best examples are electron exchange between metal complexes, for which the Marcus model was originally conceived.[1–3] However, the model may be used to treat ET in several other types of system, for example, between organic molecules, and intramolecular ET. A necessary improvement has been the introduction of the Landau–Zener approximation to include cases where the electronic coupling is small.[4] Other models for the case of a small reaction barrier and electronic coupling, which also permit the nuclei to be treated quantum mechanically, have been introduced.[5] Furthermore, Hush has introduced methods to analyze the intervalence spectrum and extract H_{ad}, which in the standard model appears as the electronic factor in the rate expression.[6]

In the Marcus model and its extensions to donor–bridge–acceptor systems, it is assumed that the bridge acts as a tunneling barrier for the electrons. Localization of the transferring electrons on the bridge is assumed not to occur. Only donor and acceptor geometries are affected by the change in number of electrons, and hence, the reorganization energy λ may be calculated for donor and acceptor systems separately. The coupling may be introduced, in fortunate cases, as a local coupling between the connecting atomic orbitals of donor and bridge and bridge and acceptor, multiplied by a transfer capability function that is a property of the bridge.[7]

Nelsen's group has shown that the rate constants for intramolecular electron transfer within several aromatic-bridged bis(hydrazine) radical cations are accurately predicted using the simple Marcus two-state model with electron transfer parameters derived from their optical spectra.[8] However, for one case (that having 9,10-anthracenediyl as the bridge), intramolecular electron transfer was much faster than predicted from the two-state model, and the optical spectrum was anomalous. Both effects are consistent with an excited state having charge mostly localized on the anthracene bridge, too close in energy to the hydrazine-localized ground states for the two-state model to be useful.[9]

In this article we apply *ab initio* and DFT methods to calculate the relevant parameters of the Marcus–Hush model for six cases shown experimentally to fit this simple model. Contrary to the ordinary Marcus–Hush model, we find that the electronic coupling derived by optical methods is much smaller than one half of the calculated energy splitting between the relevant PESs at the transition state. We believe this is due to differences in structure, especially the important angle φ, and wave function for the molecules in the relaxed, asymmetric state, and the transition state.

Methodology

All calculations were carried out using the software package *Gaussian 98*[10] with two different levels of theory, Hartree–Fock (HF) and DFT, using Becke's three-parameter hybrid functional with the correlation functional by Lee, Yang, and Parr (B3LYP).[11–13] For the HF calculations we used the basis set 3–21G and for the B3LYP calculations 6-31G*. All structures were first optimized with HF/3-21G and then reoptimized with B3LYP/6-31G*. We have used Koopmans' theorem (see below) to approximate the electronic coupling as one-half of an orbital energy difference for compounds 1–6 (see Scheme 1). Both the compounds having only one hydrazine unit attached to the bridge (only **1A** is shown), and those with two hydrazine units attached (the **B** structures shown) have been calculated.

The reorganization energy consists of two parts, the inner and outer reorganization energy, λ_i and λ_o, respectively. The former is due to changes in bond lengths and bond angles upon ET, and the latter to average reorientation of the solvent molecules. λ_i may be obtained quantum mechanically by modeling the geometrical changes of donor and acceptor during ET. Even though donor and acceptor are the same in the bis(hydrazines), the geometries are different due to charge localization in the relaxed state, making the molecules asymmetric. Monohydrazines **1A**–**6A** were used to model the geometrical changes of donor and acceptor for electron transfer within dihydrazine radical cations **1B$^+$**–**6B$^+$**. The bridges were included to account for impacts of steric hindrance. By geometry optimization of **A**^{0}
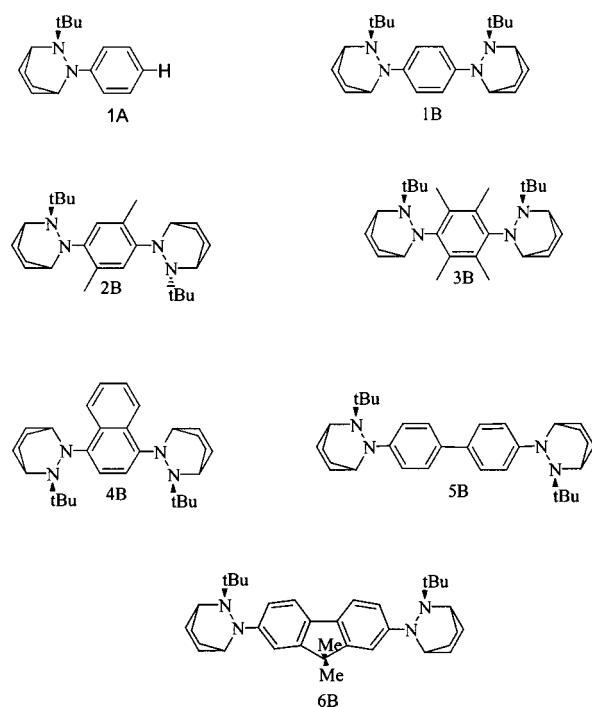
SCHEME 1. Calculated structures. Of the monohydrazines, abbreviated A, only 1A is shown. All bis(hydrazines), abbreviated B, are shown in the respective symmetry as performed on the transition state structures (see text).

and $\mathbf{A}^+$, we get the geometries of the neutral and charged hydrazine units, called N^0 and C^+, respectively. The geometries N^0 and C^+ model the geometries of donor and acceptor for the molecule in the relaxed state of the bis(hydrazine), i.e., in one of the potential wells in the Marcus model. By interchanging the charges of N^0 and C^+ without changing the geometries, which simulates a vertical transition from one of the potential wells to the excited state surface in the Marcus model, we get N^+ and C^0. λ_i is then calculated as:[14]

$$\lambda_i = \left[E(N^+) - E(C^+)\right] + \left[E(C^0) - E(N^0)\right] \quad (1)$$

where E stands for the total energy, within the Born–Oppenheimer approximation, of the corresponding geometry and charge. The first and second part of eq. (1) accounts for the energy associated with geometrical changes of donor and acceptor, respectively. The vertical transition from one of the potential wells to the excited state surface corresponds to the removal of one electron from donor to acceptor without changing the geometry. For systems like $\mathbf{B}^+$ where donor and acceptor are the same except for charge and geometry, $\Delta G = 0$ for the ET reaction, the relaxation energy from the excited

state to the potential well of the ground state surface equals λ, and eq. (1) may be used to calculate the part associated with changes in bond lengths and bond angles, λ_i. One N—Ar bond rotation, double nitrogen inversion isomer was calculated for each bis(hydrazine), that shown in Scheme 1, chosen to be of the proper symmetry to allow calculation of a delocalized transition state structure and to minimize steric interactions between the hydrazine units and the bridge. Using monohydrazines **A** to model λ_i for bis(hydrazines) **B** is an approximation that becomes better as H_{ad} becomes smaller, because the wave functions of the oxidized and reduced hydrazine units mix more as the electronic coupling increases, resulting in intermediate geometries. This effect has been seen in the X-ray crystallographic structural parameters for $\mathbf{1B}^+$ compared with $\mathbf{1A}^+$ and $\mathbf{1B}^0$, but is not evident for $\mathbf{3B}^+$, which has only 46% as large an optically determined H_{ad} value.[8b]

According to the Marcus model, ET occurs through a symmetric transition state where the electron is delocalized with equal coefficients on donor and acceptor. Let us first assume that we have isolated donor and acceptor molecular subsystem orbitals, ϕ_d and ϕ_a, respectively. Delocalized, normalized MOs with a plus and minus combination between ϕ_d and ϕ_a may be written as:

$$\phi_+ = \frac{1}{\sqrt{2}}(\phi_d + \phi_a); \qquad \phi_- = \frac{1}{\sqrt{2}}(\phi_d - \phi_a) \quad (2)$$

In the case of the bis(hydrazines), ϕ_d and ϕ_a are combinations of nitrogen lone-pair MOs. For many compounds, as well as for the bis(hydrazines), the highest occupied molecular orbital (HOMO) and the next highest occupied molecular orbital (HOMO-1) have the properties of eq. (2), with a plus and minus combination between donor and acceptor subsystem orbitals. Now looking at the many-electron wave function, it follows that the upper and lower PESs in the Marcus model correspond to the cases where the molecule is ionized from HOMO-1 and HOMO, respectively. The electronic coupling may, hence, be calculated as half the energy difference between the two PESs at the transition state. One common method is to use Koopmans' theorem,[15] where $2H_{ad}$ is approximated as an orbital energy difference between ϕ_+ and ϕ_-. This method has proved to be useful for other types of nitrogen compounds.[16]

$$I_{HOMO-1} = E_{HOMO-1}^{N-1} - E^N \approx -\varepsilon_{HOMO-1} \quad (3)$$

$$I_{HOMO} = E_{HOMO}^{N-1} - E^N \approx -\varepsilon_{HOMO} \quad (4)$$

$$I_{\text{HOMO-1}} - I_{\text{HOMO}} = E_{\text{HOMO-1}}^{N-1} - E_{\text{HOMO}}^{N-1}$$
$$= 2H_{\text{ad}} \approx \varepsilon_{\text{HOMO}} - \varepsilon_{\text{HOMO-1}} \quad (5)$$

In eqs. (3)–(5) I is ionization potential, ε orbital energy of the neutral system, E_i^{N-1} and E^N are total energies of the ionized and neutral state, respectively. In the ionized state, ionization has occurred from orbital i. This "frozen orbital" approximation assumes that the spin orbitals in the ionized and neutral states are identical, and thus neglects relaxation effects in the ionized state, when used to calculate ionization potentials. In the calculation of $2H_{\text{ad}}$, however, the expectation values of the two ionized states are used in which the local orbitals are identical, leading to favorable conditions for error cancellation. Koopmans' theorem was used for the B3LYP/6-31G* as well as for the HF/3-21G calculations. HOMO and HOMO-1 are the same obtained by these two methods as far as symmetry is concerned. Also, the appearance is the same, i.e., the two methods produce approximately the same coefficients.

The transition states $\mathbf{B}^{\ddagger}$ were modeled by selecting the desired symmetry, C_2, C_i, or C_s, respectively, and constraining the bond lengths, bond angles, and twist angles of equivalent atoms on both sides of the symmetry center to be the same during a geometry optimization of the radical cation. We chose C_s symmetry of the transition state for compounds **1B**, **3B**, **4B**, and **6B**, and for compounds **2B** and **5B** we chose C_i, and C_2, respectively. The chemical structures are shown in the chosen symmetries in Scheme 1.

Figure 1 shows a drawing of the atoms around the N—N bond of a hydrazine unit.
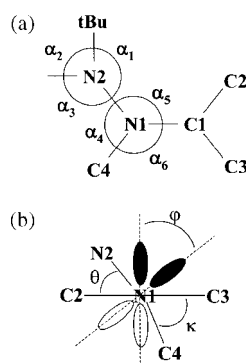

FIGURE 1. A sketch of the nitrogen group in a hydrazine unit. The view of (a) is from above, and it is used to define d, $\Delta\alpha(\text{Ar})_{\text{av}}$ and $\Delta\alpha(t\text{Bu})_{\text{av}}$ (see text). The view of (b) is to the left of (a) and along the N1—C1 bond. It is used to define the angles θ, κ, and φ (see text).

Hydrazines undergo unusually large geometry changes upon ionization. An electron is removed from an antibonding combination of the nitrogen lone pair orbitals, decreasing the bond length about 10% and increasing the p character of the orbital, flattening the oxidized hydrazine unit. As a consequence of the concomitant increase in steric interaction between the *tert*-Butyl group and the hydrogens of the aromatic bridge moiety, the aryl twist angle increases. Structural parameters that undergo large changes during ET are the bond distance between N1 and N2, called d, the dihedral angles ∠C2C1N1N2 and ∠C3C1N1C4, called θ and κ, respectively. The pyramidalities of the two nitrogen atoms also undergo large changes. These are defined using the average of the angles in Figure 1a:

$$\Delta\alpha(t\text{Bu})_{\text{av}} = 120 - \frac{\alpha_1 + \alpha_2 + \alpha_3}{3};$$
$$\Delta\alpha(\text{Ar})_{\text{av}} = 120 - \frac{\alpha_4 + \alpha_5 + \alpha_6}{3} \quad (6)$$

Because the N—N bond surrounding is not coplanar (not even for the oxidized unit), θ is not the same as the angle between the lone pair of the nitrogen attached to the aryl ring and the p-orbital of the adjacent bridge carbon, φ, which controls the magnitude of the electronic coupling. To get a reasonable value of this important parameter, φ is here defined as the average between θ and κ (see Fig. 1b). This relation is quantitatively accurate when the two NNC angles are the same, and is an excellent assumption for the structures considered here.

The activation barrier, ΔG^*, can be calculated in two ways. The first way uses the classical Marcus model. For systems where the donor and the acceptor are the same, the expression is:

$$\Delta G^* = \frac{\lambda}{4} - H_{\text{ad}} + \frac{H_{\text{ad}}^2}{\lambda} \quad (7)$$

The other way is simply to take the difference in calculated, total energy between the symmetric transition state and the relaxed, asymmetric equilibrium geometry of the cation. It should be noted that calculation of the activation barrier quantum mechanically by means of eq. (7) or as an energy difference between the two states, free energies in the Marcus model are replaced by calculated enthalpies. The structures of the relaxed cations were optimized with the same conformation of the nitrogen bonds relative the bridges as in the transition state for compounds 2 and 4, i.e., anti to the methyl groups of the bridge and the extra benzo group, re-

spectively. The conformations of the nitrogen bonds relative each other were the same as in Scheme 1 for all compounds.

Calculated Structures and Parameters

All geometry optimizations were performed using two different levels of theory: HF/3-21G and B3LYP/6-31G* (abbreviated in the tables as HF and DFT), as described earlier. The results are here presented in Tables I–IV.

Table I compares calculated structural parameters for the oxidized and reduced forms of the mono(hydrazines) and the oxidized forms of the bis(hydrazines) with X-ray structural data. Most neutral hydrazines in this series, including the neutral end of bis(hydrazines), are badly disordered by the presence of more than one N—Ar rotation and double nitrogen inversion form, and in many cases good structural parameters could not be obtained. As is clear from Table I, the twist angle θ is rather "soft," and significant differences occur even between mono- and bis(hydrazine) crystal structures.

TABLE I.

Comparison of Calculated and X-ray Structural Parameters for Oxidized and Reduced Hydrazine Units.

Parameter	Bridge Cmpd Type[a]	-PH- $1A^0/1A^+$	-XY- $2A^0/2A^+$	-DU- $3A^0/3A^+$	-NA- $4A^0/4A^+$	-BI- $5A^0/5A^+$	-FL- $6A^0/6A^+$
d (Å)	HF	1.46/1.35	1.47/1.35	1.47/1.35	1.47/1.35	1.46/1.35	1.46/1.35
	DFT	1.45/1.36	1.46/1.36	1.46/1.36	1.47/1.36	1.45/1.36	1.45/1.37
	X-ray	1.46[b]/1.35[c]	/1.35[e]	/1.37[f]1.36[g]	/1.35[j]	1.44[k]/1.35[m]/1.36[n]	
θ (deg)	HF	17/36	25/54	35/82	26/59	17/64	18/64
	DFT	12/39	21/42	31/60	23/42	10/34	12/39
	X-ray	10[b]/37&43[c]	/47[e]	/53[f]52[g]	/48[j]	15[k]/48[m]/29[n]	
κ (deg)	HF	69/81	77/81	78/85	79/85	68/81	69/81
	DFT	64/69	74/74	76/77	76/73	62/64	64/62
	X-ray	65[b]/70&76[c]	/73[e]	/74[f]75[g]	/81[j]	71[k]/83[m]/59[n]	
φ (deg)	HF	43/72	51/68	57/84	53/72	43/73	44/73
	DFT	38/54	48/58	54/69	50/58	36/49	38/51
	X-ray	37[b]/53&60[c]	/57[e]	/64[f,g]	/65[j]	43[k]/65[m]/44[n]	
$\Delta\alpha(t\text{Bu})_{av}$	HF	5.9/0.4	6.0/0.2	6.5/0.1	5.8/0.2	5.9/0.3	5.9/0.3
	DFT	6.1/0.9	6.1/0.8	6.5/1.1	6.0/0.9	6.0/1.0	6.0/2.9
	X-ray	6.9[b]/0.7&0.9[c]	/0.9[e]	/1.2[f]1.5[g]	/0.9[j]	7.1[k]/0.8[m]/1.2[n]	
$\Delta\alpha(\text{Ar})_{av}$	HF	7.2/1.3	7.3/2.2	5.1/0.1	7.5/2.3	7.1/1.2	7.2/1.2
	DFT	7.0/2.6	7.2/2.8	5.1/1.2	7.5/3.0	6.9/2.6	6.9/1.8
	X-ray	8.0[b]/2.8&3.0[c]	/2.5[e]	/1.5[f,g]	/3.1[j]	8.2[k]/3.6[m]/2.8[n]	

Parameter	Cmpd Type[a]	$1B^+$ 0/1+	$2B^+$ 0/1+	$3B^+$ 0/1+	$4B^+$ 0/1+	$5B^+$ 0/1+	$6B^+$ 0/1+
d (Å)	HF	1.46/1.35	1.47/1.35	1.47/1.35	1.47/1.35	1.46/1.35	1.46/1.35
	X-ray	1.45[d]/1.36[d]		1.45[h]/1.35[h]			
θ (deg)	HF	11/65	22/56	34/86	24/54	16/67	18/69
	X-ray	6[d]/30[d]		22-29[h]/59[h]			
κ (deg)	HF	61/81	74/80	76/86	76/82	67/83	69/84
	X-ray	60[d]/65[d]		70-78[h]/73[h]			
φ (deg)	HF	36/73	48/68	55/86	50/68	41/75	44/77
	X-ray	33[d]/48[d]		46-53[h]/66[h]			

TABLE I.
(Continued)

Parameter	Cmpd Type[a]	1B$^+$ 0/1+	2B$^+$ 0/1+	3B$^+$ 0/1+	4B$^+$ 0/1+	5B$^+$ 0/1+	6B$^+$ 0/1+
$\Delta\alpha(t\text{Bu})_{av}$	HF	5.9/0.3	6.0/0.2	6.5/0.0	6.1/0.2	6.0/0.3	6.0/0.3
	X-ray	7.8^d/1.3^d		6-8^h/1.0^h			
$\Delta\alpha(\text{Ar})_{av}$	HF	6.4/1.2	7.0/2.0	4.8/0.0	7.2/2.1	7.0/1.2	7.0/1.1
	X-ray	6.4^d/3.8^d		6-7^h/1.0^h			

[a] HF means HF/3-21G calculations, DFT means B3LYP/6-31G* calculations, and X-ray means X-ray crystallographic structure determinations, either on monohydrazines **A** or dihydrazines **B**. Structural data for monohydrazines and neutral or dicationic dihydrazines, for which the hydrazine units are the same, are shown with the calculated **A** structures, and dihydrazine radical cations, where the hydrazine units are different, are shown with the **B**$^+$ structures.
[b] **1B**^{0}.[8b]
[c] **1A**$^+$(CCH)$_4$B$^-$ and **1A**$^+$NO$_3^-$.[8b]
[d] **1B**$^+$Ph$_4$B$^-$.[8b]
[e] **2B**$^{2+}$(Ph$_4$B$^-$)$_2$2MeCN.[8b]
[f] **3A**$^+$NO$_3^-$.[8b]
[g] **3B**$^{2+}$(Ph$_4$B$^-$)$_2$.[8b]
[h] **3B**$^+$Ph$_4$B$^-$.
[j] **4A**$^+$SbF$_6^-$.
[k] **5B**^{0}.
[m] **5A**$^+$SbF$_6^-$0.5Et$_2$O.
[n] **5B**$^{2+}$(SbF$_6^-$)$_2$MeCN.

The HF calculations predict the oxidized forms to be too flat compared to crystal structures, which make $\Delta\alpha$ too small and θ too large, and the smaller +1 form of θ obtained for the sterically more hindered 2 and 4 than for 1, 5, and 6 is obviously incorrect, but the DFT structures appear to be much more realistic. The principal problem with the DFT structures of Table I appears to be slightly flatter neutral

TABLE II.
Calculated Structural Parameters for Bis(hydrazine) Electron Transfer Transition States.

Parameter	Bridge Type[a]	-PH- 1B‡	-XY- 2B‡	-DU- 3B‡	-NA- 4B‡	-BI- 5B‡	-FL- 6B‡
d (Å)	HF	1.45	1.45	1.45	1.45	1.45	1.45
	DFT	1.41	1.41	1.41	1.42	1.42	1.42
θ (deg)	HF	10	20	32	19	7.7	8.7
	DFT	17	25	39	25	16	16
κ (deg)	HF	42	56	59	59	46	48
	DFT	53	64	67	65	53	54
φ (deg)	HF	26	38	46	39	27	28
	DFT	35	45	53	45	35	35
$\Delta\alpha(t\text{Bu})_{av}$	HF	5.8	5.8	5.6	5.9	5.8	5.8
	DFT	5.2	4.9	4.7	5.0	5.2	5.3
$\Delta\alpha(\text{Ar})_{av}$	HF	2.5	3.4	1.9	4.0	3.6	4.0
	DFT	3.3	3.8	2.2	4.1	3.6	3.7

[a] HF means HF/3-21G calculations, DFT means B3LYP/6-31G* calculations.

hydrazine units than found experimentally. Similar structural information appears for the calculated transition state structures in Table II. The d values and NN, Ar twist angles are closer to those for the neutral hydrazines than the cationic ones, but pyramidalities at the aryl-bound nitrogen are closer to those for the cationic hydrazine units. These structures appear consistent with significant contributions from conjugated quinonoid-like N=Ar=N geometries. The charge and spin distributions (not presented here) of the optimized transition state structures are symmetric for all compounds using both methods.

Table III contains electron transfer parameters calculated from the above structures.

The λ_i values are calculated from the monohydrazines **A** in both oxidation states using eq. (1). The values calculated by HF are larger than the experimental λ_{opt} values, which include the solvent reorganization energy as well as λ_i. This presumably occurs because of the larger geometry changes upon electron removal obtained in the calculations (see Table I), than actually occurs. The DFT λ_i values are more realistic, although they also may be slightly high, if the conventional λ_s estimates of ~9 kcal/mol for the five-bond-bridged $\mathbf{1B^+}$–$\mathbf{4B^+}$ and 20 kcal/mol for $\mathbf{5B^+}$ and $\mathbf{6B^+}$ are close to being accurate.

The calculated electronic couplings, obtained from the $\mathbf{B^{\ddagger}}$ structures, also appear in Table III. Much smaller H_{ad} values (29–40% as large) are obtained using the more realistic DFT than HF calculations. The simplest test of the reliability of the calculated λ and H_{ad} values obtained appears to be to use F, the fraction of the $\lambda/4$ activation barrier ΔG^* at small H_{ad} that remains for the H_{ad} that is present, which one of us recently pointed out is obtained by rearranging the two-state model eq. (7) as eq. (8).[17] In eq. (8) $\Delta = 2H_{ad}$.

$$F = \left(1 - \frac{\Delta}{\lambda}\right)^2. \qquad (8)$$

As can be seen in Table III, the F_{calc} values using HF are unreasonably large, the calculated H_{ad} even being so large for $\mathbf{1B^{\ddagger}}$ that $\mathbf{1B^+}$ would be delocalized at the λ value calculated. The DFT F_{calc} values are much more reasonable, although they are still significantly smaller than the experimental F_{opt} values.

We have also calculated the structures of the relaxed, asymmetric cations of the six bis(hydrazine) radical cations. This was done to calculate the activation energy by taking the difference in total energy between the transition state and the relaxed cation. Another reason was to see how well the monomers model the dimers. The B3LYP/6-31G* calculations carried out in a straightforward way,

TABLE III.

Comparison of Calculated and Optical Vertical Reorganization and Electronic Couplings (kcal/mol).

Quantity	Bridge Method[a]	-PH- $\mathbf{1A^{0/+}}$	-XY- $\mathbf{2A^{0/+}}$	-DU- $\mathbf{3A^{0/+}}$	-NA- $\mathbf{4A^{0/+}}$	-BI- $\mathbf{5A^{0/+}}$	-FL- $\mathbf{6A^{0/+}}$
λ_i	HF	45.8	46.3	50.6	67.2	42.1	46.0
	DFT	31.5	31.6	34.4	28.8	26.3	21.1
$\lambda_{opt} = \lambda_i + \lambda$	optical[8]	37.8	41.2	40.7	36.4	43.7	38.9
		$\mathbf{1B^{\ddagger}}$	$\mathbf{2B^{\ddagger}}$	$\mathbf{3B^{\ddagger}}$	$\mathbf{4B^{\ddagger}}$	$\mathbf{5B^{\ddagger}}$	$\mathbf{6B^{\ddagger}}$
H_{ad}	HF	30.1	26.2	21.5	30.0	21.8	23.4
	DFT	11.9	9.1	6.3	10.6	6.4	7.6
H_{ad}	optical[8]	7.2	4.9	3.3	4.3	3.6	4.1
F_{calc}[b]	HF	—	0.003	0.08	0.05	0.09	0.09
	DFT	0.17	0.30	0.32	0.19	0.53	0.40
F_{opt}[c]	optical[8]	0.38	0.58	0.70	0.58	0.70	0.62

[a] HF means HF/3-21G calculations, DFT means B3LYP/6-31G* calculations, and optical[8] means numbers extracted from the optical spectrum as described in ref. 8.

[b] Fraction of the $\lambda/4$ diabatic surface crossing point barrier remaining after inclusion of electronic coupling in a two state model using $F_{calc} = (1 - \Delta_{calc}/\lambda_{calc})^2$, employing conventional values of $\lambda_s = 9$ kcal/mol for the five-bond-bridged systems **1–4** and 20 kcal/mol for the nine-bond-bridged systems **5** and **6**.

[c] Fraction of the $\lambda/4$ barrier remaining after electronic coupling effects are including in a two state model using $F_{opt} = (1 - \Delta_{opt}/\lambda_{opt})$.

Vibrational Reorganizational Barriers (kcal/mol) for Intramolecular ET Calculated Using the Enthalpy Difference between HF/3-21G Structures for $B^{\ddagger}$ and B^{+}.

Compound	Barrier
$1B^+$	5.8
$2B^+$	10.8
$3B^+$	18.4
$4B^+$	7.3
$5B^+$	13.0
$6B^+$	12.5

failed to localize the electron properly. This was concluded when the optimized structures of the relaxed cations were examined. The difference in d, θ, $\alpha(t\text{Bu})_{av}$, and $\alpha(\text{Ar})_{av}$ for donor and acceptor were too small to model the localization, which is seen in the crystal structures mentioned earlier. Previous studies of small cations have shown cases where delocalization is overestimated by DFT methods.[18–20]

The HF/3-21G B^+ structures, which are properly localized, are shown at the end of Table I. The θ values for the oxidized hydrazine units of both A^+ and B^+ of **2** and **4** are smaller than those for the less hindered **1**, **5**, and **6**, which is incorrect, and the X-ray structures indicate that the principal problem is that too large twists are calculated for the less hindered systems. The barriers calculated from the HF/3-21G $B^{\ddagger}$ and B^+ enthalpy differences are shown in Table IV. They are far larger than the experimental barriers measured by ESR,[8] presumably because the structures are rather poor.

Discussion

The π-systems used as bridges are directly attached to the nitrogen atoms of the hydrazine units. In the neutral molecule the hydrazine N—N bonds are single bonds where the antibonding as well as the bonding combination of the lone pair MOs on the nitrogens are fully occupied. When the system is ionized from the antibonding combination, half a π bond is introduced in one of the hydrazine units, shortening the N—N bond and forcing the NN group with four bonded atoms to be as planar as possible, decreasing both $\Delta\alpha(t\text{Bu})_{av}$ and $\Delta\alpha(\text{Ar})_{av}$. This produces increased steric hindrance between the bridge and especially the tertiary butyl group,

which causes the angle θ to be larger for the ionized unit. The direct relation between θ and φ (see above for definition) also causes φ to be larger for the ionized unit. The total coupling between donor and acceptor is proportional to $\eta_1\eta_2 = \beta_1\beta_2\cos(\varphi_1)\cos(\varphi_2)$. 1 and 2 are the indexes for the coupling matrix elements between the nitrogens attached to the bridge and the adjacent bridge carbon atoms at the donor and acceptor endpoints of the bridge. Because the electronic coupling may be approximately written:[7]

$$H_{ad} = \eta_1\eta_2 \sum_{\nu} \frac{c_{1\nu}c_{n\nu}}{b_\nu - a} \qquad (9)$$

in eq. (9), H_{ad} is proportional to $\cos(\varphi_1)\cos(\varphi_2)$. The summation runs over bridge MOs with energy b_ν. a is the orbital energy of the transferring electron and $c_{1\nu}$ and $c_{n\nu}$ coefficients at the end points of the bridge. η_1 and η_2, finally, are coupling matrix elements between the nitrogens and the bridge carbons, which may be written as $\eta = \beta\cos(\varphi)$, where β is Hückel $\beta \approx 2$ eV. Our calculations indicate that the ET reaction for these compounds involves a decrease of φ, especially for the ionized hydrazine unit, at the transition state compared to the relaxed, asymmetric state. This is consistent with the ET reaction mechanism for these compounds. When the conjugation, or charge, is shared between both units, the planarity around the nitrogens is decreased, and consequently, the angles θ and φ are decreased. Our calculations indicate that the value of $\Delta\alpha(t\text{Bu})_{av}$ for both units at the transition state is about the same as for the neutral unit at the relaxed, asymmetric state. This is the reason for the lowered values of θ and φ, because both are controlled by $\Delta\alpha(t\text{Bu})_{av}$. According to eq. (9), the structure of the transition state would explain the discrepancy between calculated and experimental results of the electronic coupling. At the relaxed, asymmetric state φ is 10–40° larger, depending on compound, for the ionized hydrazine unit. Consequently, the product $\cos(\varphi_1)\cos(\varphi_2)$ is smaller for this state than at the transition state where the electron is delocalized and φ is small for both hydrazine units.

Nelsen's group have investigated these compounds experimentally and demonstrated that a coupling can be obtained by optical methods, for which the measurements are performed at the geometry of the relaxed, asymmetric state. Using parameters derived by optical methods, rate constants have been calculated which fit with good agreement to ones measured by ESR. For small couplings the intervalence transition is a charge trans-

fer transition where the intensity depends linearly on the admixture of wave function corresponding to the other location of the electron. The expression for deriving the electronic coupling from spectra is:[6]

$$H_{ad} = \frac{2.06 \times 10^{-2}}{R} \cdot (\lambda \cdot \varepsilon_{max} \cdot \Delta v_{1/2})^{1/2} \qquad (10)$$

This equation relates spectral features to the coupling. R is the electron transfer distance, λ is the reorganization energy, ε_{max} is the extinction coefficient at the band maximum and $\Delta v_{1/2}$ is the bandwidth at half-height. The geometry belongs to the geometry of the relaxed, asymmetric dihydrazine cation radical, with the electron localized essentially to one of the sites. According to our calculations, this geometry corresponds to the acceptor-bridge angle being 10–40° larger than the donor-bridge angle, depending on the compound in question (see Table I). In the Marcus model the rate expression is:[3]

$$k = v_n \mu \exp(-\Delta G^*/k_B T) \qquad (11)$$

where v_n is the frequency of the activating vibration, ΔG^* is the activation barrier, k_B is Boltzmanns constant, and T is the absolute temperature. μ is the electronic transmission coefficient, defined as:

$$\mu = \frac{2[1 - \exp(-v_{el}/2v_n)]}{2 - \exp(-v_{el}/2v_n)} \qquad (12)$$

$$v_{el} = \frac{2\pi}{\hbar} H_{ad}^2 \sqrt{\frac{1}{4\pi \lambda k_B T}} \qquad (13)$$

In eq. (13) λ is the reorganization energy and H_{ad} is the electronic coupling. Even for the smaller couplings obtained experimentally, μ is very close to unity (choosing $hv_n = 800$ cm^{-1})[8] and ET occurs adiabatically. Hence, the rate dependence on H_{ad} is not explicit, it appears in the calculation of ΔG^* using eq. (7). This preserves the good agreement with rate constants measured by ESR, although the electronic coupling is increased at the transition state compared to the relaxed state.

Even though the calculations are approximations, we have seen a trend indicating that φ is lowered for both hydrazine units at the transition state. In view of these calculations, this would mean that the coupling is not constant during the ET process, i.e., the coupling derived according to eq. (10), corresponding to the relaxed, asymmetric state, is smaller than the energy separation at the transition state. However, the reaction coordinate in the Marcus model also includes the solvent, which is not included in our calculations. When comparing the calculated geometries to crystal structures we

find reasonable agreement for all structural parameters, using both methods, except for θ. It is clear that θ is a soft parameter, and the calculated and crystal structure values might differ significantly from the weighted average that affect the optical spectrum.

Conclusions

In symmetric systems the Marcus model describes electron transfer in terms of two parameters, reorganization energy λ, and electronic coupling H_{ad}. With this model a good description is obtained for self-exchange in organic molecules in most cases using spectroscopic data for the electronic factor. In this article we have applied standard calculational procedures to investigate ET in compounds **1B$^+$**–**6B$^+$**. However, we find that the calculation of H_{ad} is not as straightforward for bis(hydrazines) bridged by π-systems as for rigid systems that cannot twist between the charge-bearing units and the bridge.

The calculations performed in this paper indicate that the coupling cannot be assumed constant during the ET process, which is a necessity when applying eq. (10). Instead, it might be increased at the transition state relative to that of the relaxed state. We believe that some of the discrepancy between the calculated and experimentally obtained values of H_{ad} can be explained by differences in structure and wave function between the symmetric ET transition state and the asymmetric, relaxed state. Spectral properties, which have been used traditionally to calculate the electronic factor according to eq. (10), correspond to the latter state, where φ is large for the ionized hydrazine unit. At the transition state, where we have calculated H_{ad} using Koopmans' theorem, φ is smaller for both units. This small value of φ explains the large values of the calculated electronic couplings, compared to the measured ones, according to eq. (9). The numbers obtained for the electronic coupling by Koopmans' theorem may be questioned to some degree, especially those produced by HF/3-21G, which appears to be a rather crude approximation. The bis(hydrazines) studied in this article by *ab initio* and DFT methods are charge localized compounds, which is shown in the crystal structures. When reorganization energies and electronic factors are calculated using HF/3-21G we get $\Delta > \lambda$. This is inconsistent for charge localized compounds according to the two-state, one-dimensional Marcus model. Perhaps more reasonable results of these parameters

are produced by B3LYP/6-31G* calculations in this sense. On the other hand, less localization is obtained by the latter method than corresponding to the measured localization in the crystal.

However, the qualitative features remain in both methods. The lowering of φ at the transition state is consistent with the mechanism for ET along the reaction path for these compounds.

Addendum

When the preparation of this article was in progress, an important article by Fernández et al.[21] was published where an *ab initio* study on a model system similar to the one studied here, was carried out. The compound studied in that article, however, differs from those studied experimentally and calculated here because the ET proceeds through a bridge-oxidized state, a third surface with the electron localized on the bridge.

References

1. Marcus, R. A. Ann Rev Phys Chem 1960, 15, 155.

2. Brunschwig, B. S.; Logan, J.; Newton, M. D.; Sutin, N. J Am Chem Soc 1980, 102, 5798.

3. Brunschwig, B. S.; Creutz, C.; Maccartney, D. H.; Sham, T. K.; Sutin, N. Faraday Discuss Chem Soc 1982, 74, 113.

4. Sutin, N. Bioorganic Chemistry; Eichhorn, G. L., Ed.; American Elsevier: New York, 1973, p. 611, vol. 2.

5. Ulstrup, J.; Jortner, J. J. Chem Phys 1975, 63, 4358.

6. Hush, N. S. Prog Inorg Chem 1967, 8, 391; Coord Chem Rev 1985, 64, 135.

7. Larsson, S. J Am Chem Soc 1981, 103, 4034.

8. (a) Nelsen, S. F.; Ismagilov, R. F.; Gentile, K. E.; Powell, D. R. J Am Chem Soc 1999, 121, 7108; (b) Nelsen, S. F.; Ismagilov, R. F.; Powell, D. R. J Am Chem Soc 1997, 119, 10213.

9. Nelsen, S. F.; Ismagilov, R. F.; Powell, D. R. J Am Chem Soc 1998, 120, 1924.

10. Frisch, M. J.; Trucks, G. W.; Schlegel, H. B.; Scuseria, G. E.; Robb, M. A.; Cheeseman, J. R.; Zakrzewski, V. G.; Montgomery, J. A., Jr.; Stratmann, R. E.; Burant, J. C.; Dapprich, S.; Millam, J. M.; Daniels, A. D.; Kudin, K. N.; Strain, M. C.; Farkas, O.; Tomasi, J.; Barone, V.; Cossi, M.; Cammi, R.; Mennucci, B.; Pomelli, C.; Adamo, C.; Clifford, S.; Ochterski, J.; Petersson, G. A.; Ayala, P. Y.; Cui, Q.; Morokuma, K.; Malick, D. K.; Rabuck, A. D.; Raghavachari, K.; Foresman, J. B.; Cioslowski, J.; Ortiz, J. V.; Baboul, A. G.; Stefanov, B. B.; Liu, G.; Liashenko, A.; Piskorz, P.; Komaromi, I.; Gomperts, R.; Martin, R. L.; Fox, D. J.; Keith, T.; Al-Laham, M. A.; Peng, C. Y.; Nanayakkara, A.; Gonzalez, C.; Challacombe, M.; Gill, P. M. W.; Johnson, B.; Chen, W.; Wong, M. W.; Andres, J. L.; Gonzalez, C.; Head-Gordon, M.; Replogle, E. S.; Pople, J. A. Gaussian 98, Revision A.7; Gaussian, Inc.: Pittsburgh, PA, 1998.

11. Becke, A. D. Phys Rev A 1988, 38, 3098.

12. Lee, C.; Yang, W.; Parr, R. G. Phys Rev B 1988, 37, 785.

13. Vosko, S. H.; Wilk, L.; Nusair, M. Can J Phys 1980, 58, 1200.

14. Nelsen, S. F.; Blackstock, S. C.; Kim, Y. J Am Chem Soc 1987, 109, 677.

15. Koopmans, T. A. Physica 1934, 1, 104.

16. (a) Braga, M.; Larsson, S. J Phys Chem 1992, 96, 9218; (b) Nelsen, S. F.; Tran, H. Q.; Nagy, M. A. J Am Chem Soc 1998, 120, 298.

17. Nelsen, S. F. Chem Eur J 2000, 6, 581.

18. Bally, T.; Sasty, G. N. J Phys Chem A 1997, 101, 7923.

19. Braïda, B.; Hilberty, P. C.; Savin, A. J Phys Chem A 1998, 102, 7872.

20. Sodupe, M.; Bertran, J.; Rodríguez-Santiago, L.; Baerends, E. J. J Phys Chem A 1999, 103, 166.

21. Fernández, E.; Blanchafort, L.; Olivucci, M.; Robb, M. A. J Am Chem Soc 2000, 122, 7528.